Published in final edited form as:
J Neurochem. 2010 October ; 115(1): 168–177. doi:10.1111/j.1471-4159.2010.06913.x.

Involvement of ceramide in ethanol-induced apoptotic neurodegeneration in the neonatal mouse brain

Mariko Saito[1,3], **Goutam Chakraborty**[1], **Medha Hegde**[1], **Jason Ohsie**[1], **Sun-Mee Paik**[1], **Csaba Vadasz**[1,3], and **Mitsuo Saito**[2,3]

[1] Division of Neurochemisty, The Nathan S. Kline Institute for Psychiatric Research, Orangeburg, New York

[2] Division of Analytical Psychopharmacology, The Nathan S. Kline Institute for Psychiatric Research, Orangeburg, New York

[3] Department of Psychiatry, New York University Langone Medical Center, New York, New York

Abstract

Acute administration of ethanol to 7-day-old mice is known to cause robust apoptotic neurodegeneration in the brain. Our previous studies have shown that such ethanol-induced neurodegeneration is accompanied by increases in lipids including ceramide, triglyceride, cholesterol ester, and N-acyl phosphatidylethanolamine in the brain. In this study, the effects of ethanol on lipid profiles as well as caspase-3 activation were examined in the cortex, hippocampus, cerebellum, and inferior colliculus of the P7 mouse brain. We found that the cortex, hippocampus, and inferior colliculus, which showed substantial caspase-3 activation by ethanol, manifested significant elevations in ceramide, triglyceride, and N-acylphosphatidylethanolamine. In contrast, the cerebellum, with the least caspase-3 activation, failed to show significant changes in ceramide and triglyceride, and exhibits much smaller increases in N-acyl phosphatidylethanolamine than other brain regions. Ethanol-induced increases in cholesterol ester were observed in all brain regions tested. Inhibitors of serine palmitoyltransferase effectively blocked ethanol-induced caspase-3 activation as well as elevations in ceramide, cholesterol ester, and N-acyl phosphatidylethanolamine. Immunohistochemical studies indicated that the expression of serine palmitoyltransferase was mainly localized in neurons and was enhanced in activated caspase-3-positive neurons generated by ethanol. These results indicate that *de novo* ceramide synthesis has a vital role in ethanol-induced apoptotic neurodegeneration in the developing brain.

Keywords

ethanol; apoptotic neurodegeneration; ceramide; serine palmitoyltransferase; triglycerides; caspase-3 activation

Introduction

Rodents exposed to ethanol during sensitive periods of brain development manifest neuropathological conditions similar to those of the human fetal alcohol spectrum disorders (FASD). Specifically, ethanol triggers apoptotic neurodegeneration in the newborn rodent

Address correspondence and reprint requests to: Mariko Saito, The Nathan S. Kline Institute for Psychiatric Research, 140 Old Orangeburg Rd. Orangeburg, NY 10962, Phone: (845), 398-5537 Fax: (845) 398-5531, marsaito@nki.rfmh.org.
Laboratory of Neurobehavior Genetics and Division of Analytical Psychopharmacology The Nathan S. Kline Institute for Psychiatric Research and New York University Langone Medical Center, Orangeburg, NY 10962 Phone: (845) 398-5537 Fax: (845) 398-5531

brain during the period of rapid synaptogenesis that corresponds to the last trimester of pregnancy and the following several years after birth in humans (Ikonomidou et al., 2000; Olney et al., 2002). Such ethanol-induced neuronal loss in rodents may partially explain the pathophysiology of FASD-like conditions. This rodent model for FASD has been widely used to elucidate mechanisms of ethanol-induced neurodegeneration (Carloni et al., 2004; Han et al., 2006; Young et al., 2005), which shows apoptotic profiles such as caspase-3 activation (Olney et al., 2002). We previously have demonstrated that ethanol-induced neurodegeneration in 7-day-old (postnatal day 7, P7) mice is accompanied by increases in lipids, such as ceramide, triglyceride (TG), cholesterol ester (ChE), and N-acyl phosphatidylethanolamine (NAPE) in the brain (Saito et al., 2007a). Time course studies indicate that TG and ceramide increase significantly between 4 h and 8 h after ethanol exposure when robust caspase-3 activation occurs in the forebrain, while ChE and NAPE increase significantly at later time points (~24 h after ethanol exposure). We also have observed that ethanol inhibits AMP-activated protein kinase and activates acetyl-CoA carboxylase, suggesting that ethanol induces lipogenesis and leads to the ceramide elevation (Saito et al., 2007a). Ceramide, which has been shown as a pro-apoptotic mediator in many cell types (Pettus et al., 2002) including neurons (Goswami and Dawson, 2000; Jana et al., 2009), may trigger apoptosis in the P7 mouse brain treated with ethanol.

In the present study, we have evaluated further the involvement of ceramide in ethanol-induced neurodegeneration in the P7 mouse brain. First we examined the relationship between ethanol-induced apoptotic neurodegeneration and changes in lipids in the cortex, hippocampus, cerebellum, and inferior colliculus. Although ethanol induces robust apoptotic neurodegeneration in many brain areas, the frontal, parietal, cingulate, occipital, and retrosplenial cortices, thalamus, caudate putamen, subiculum, and hippocampus (CA1 layer) are among the most severely affected regions in the forebrain of P7 mice (Olney et al., 2002; Saito et al., 2007b). The cerebellum is less vulnerable to ethanol in P7 rodents although the region is more sensitive to ethanol during the early neonatal period (Dikraninan et al., 2005; Siler-Marsiglio et al., 2006). In the brainstem, the inferior colliculus appears to be most affected by ethanol at P6 (Dikraninan et al., 2005). We hypothesized that ethanol-induced changes in ceramide metabolism may vary among these brain regions where the severity of neurodegeneration differs. Apoptotic neurodegeneration was assessed by caspase-3 activation because previous studies indicated that cleaved caspase-3 (CC3) formation, which peaks 8 h after ethanol exposure, was observed mainly in neurons and was followed by neurodegeneration detected by silver staining (Olney et al., 2002). Caspase-3 activation was measured by increased expression of CC3 and caspase-cleaved tau (Ctau). It has been shown that Ctau is expressed in the cell soma of CC3-positive neurons as well as in the degenerating processes (dendrites/axons) (Saito et al., 2010).

We then examined the effects of inhibitors of serine palmitoyltransferase (SPT) on the ethanol-induced lipid elevation and capsase-3 activation. SPT is a rate-limiting enzyme for sphingolipid synthesis (Williams et al., 1984), and the inhibitors, such as ISP-1 (myriocin) and L-cycloserine (LCS), have been used to evaluate the importance of *de novo* ceramide synthesis in the various apoptotic pathways in cultured neurons (Cutler et al., 2002; Cutler et al., 2004; Herget et al., 2000; Kang et al., 2009; Saito et al., 2005). Finally, we studied the effects of ethanol on the cellular localization and expression of SPT. Results of these studies indicate the involvement of *de novo* ceramide synthesis and SPT in ethanol-induced apoptotic neurodegeneration in the developing brain.

Materials and Methods

Animals

C57BL/6By mice were maintained at the Animal Facility of Nathan S. Kline Institute for Psychiatric Research. All procedures followed guidelines consistent with those developed by the National Institute of Health and the Institutional Animal Care and Use Committee of Nathan S. Kline Institute.

Experimental Procedure

An ethanol treatment paradigm, which induces robust neurodegeneration in P7 C57BL/6 mice (Olney et al., 2002), was followed using P7 C57BL/6By mice. Each mouse in a litter was assigned to the saline or ethanol group. The mice in the saline and ethanol groups were injected subcutaneously with saline or ethanol (2.5 g/kg, 20% solution in sterile saline) twice at 0 h and 2 h. For SPT inhibitor experiments, ISP-1 (myriocin, 2 μl, 1mg/ml in 1% DMSO in saline) (Sigma, St. Louis, MO, USA) and L-cycloserine (LCS, 2 μl, 10 mg/ml in saline) (Sigma) were administered by the intracerebroventricular (icv) injection as described (Sadakata et al., 2007) 1 h before the first saline/ethanol injection. LCS (40 mg/kg, 2 mg/ml in saline) was also administered by intraperitoneal (ip) injections twice 1 h before and 1 h after the first saline/ethanol injection. Otherwise, mice were kept with the dams until brains were removed 8 to 24 h after the first saline/ethanol injection and processed for lipid analyses, immunohistochemical staining, and immunoblotting as described below. Four to ten animals were used for each data point.

Lipid analysis

Lipid analysis was performed as described previously (Saito et al., 2007a). Briefly, brain regions (the cortex, cerebellum, hippocampus, and inferior colliculus) were dissected out and placed immediately in ice-cold chloroform/methanol (1:1) solution to extract total lipids. For analyzing TG and ChE, the total lipid fraction was applied to a high-performance thin layer chromatography (HPTLC) plate, and developed first in diethylether/hexane/acetic acid (35:65:2), and then in diethylether/hexane/acetic acid (2:98:1) (Saito et al., 1987). For measuring ceramide and NAPE, 100 μl of chloroform and 75 μl of water were added to 200 μl of the total lipid fraction and centrifuged (Folch partitioning). The lower phase was applied to an HPTLC plate and developed first in a solvent of chloroform/methanol (2:1), then in a solvent of an upper phase of cyclohexane/ethylacetate/water/acetic acid (15:40:50:20). Sphingomyelin (SM) was separated from other lipids on an HPTLC plate using a solvent of chloroform/methanol/acetic acid/water (50:35:8:4). For ganglioside analysis, the upper phase obtained by the Folch partitioning of the total lipid fraction was applied to a C18 Sep-Pak cartridge. The ganglioside fraction eluted by methanol was dried, dissolved in chloroform/methanol (1:1), and applied to a HPTLC plate, which was developed by chloroform/methanol/0.25% KCl (5:4:1) (Ledeen and Yu, 1982). The plates were stained with an orcinol reagent for gangliosides, and with a solution consisting of 0.03% Coomassie Brilliant Blue, 20% methanol, and 0.5% acetic acid (Nakamura and Handa, 1984) for all other lipids. The stained HPTLC plates including standard lipids with several concentrations were scanned with the Odyssey infrared imaging system (LI-COR Biosciences, Lincoln, NE, USA) and analyzed by Multi Gauge ver.2.0 (Fujifilm USA Medical Systems, Stamford, CT, USA).

Immunohistochemistry

Eight to 24 hours after the first ethanol injection, mice were perfused with a solution containing 4% paraformaldehyde and 4% sucrose in cacodylate buffer (pH 7.2), and the heads were further fixed in the perfusion solution overnight. Then, brains were removed,

transferred to phosphate buffered saline solution, and kept at 4oC for 2–5 days until sectioned with a vibratome into 50 μm thick sections. The free-floating sections were immunostained using anti-cleaved caspase-3 (Asp175) antibody (Cell Signaling Technology, Danvers, MA, USA), anti-cleaved tau antibody (clone C3, Millipore, Billerica, MA, USA), anti-NeuN (MAB 377, Upstate, Temecula, CA, USA) antibody, and anti-SPT (subunit 2) antibody (Cayman Chemical Company, Ann Arbor, MI, USA), either by the ABC method (Vectastain ABC Elite Kit, Vector Labs, Burlingame, CA, USA) with a peroxidase substrate (DAB) kit (Vector Labs) or by a dual immunofluorescence method as described previously (Saito et al., 2007b; Saito et al., 2010). For dual labeling with anti-SPT antibody and anti-CC3 antibody, cleaved caspase-3 antibody conjugated with Alexa Fluor 488 (Cell Signaling Technology) was used. The first antibodies were omitted from reactions as a control. Also, pre-incubation with blocking peptides for anti-cleaved caspase-3 (Cell Signaling Technology), anti-C-tau antibody (CSSTGSEDMVD, GenScript, Piscataway, NJ, USA), and anti-SPT antibody (Cayman) blocked the immunostaining with these antibodies completely. For Fluoro-Jade C (Millipore) staining, brain vibratome sections obtained as described above were mounted onto gelled slides and were processed according to the manufacturer's instruction. The extent of neurodegeneration detected by Fluoro-Jade C staining was quantified in the cingulate and retrosplenial cortices. The number of stained cells in each area of interest (AOI) and the area of AOI were measured using the Image-Pro software version.4.5 (MediaCybernetics, Silver Spring, MD). The boundary of the cingulate and retrosplenial cortices was defined in accordance with Atlas of the developing mouse brain at E17.5, P0, and P6 (Paxinos et al., 2007). The Fluoro-Jade C appeared to stain not only irregular-shaped degenerating cell bodies but also other structures such as fragmented axons and dendrites. For quantification, only the degenerating cell bodies were counted. Automatic cell counting after correction (splitting adjacent cells and excluding artifacts) gave similar results to those of manual counting. The extent of neurodegeneration was expressed as the number of Fluoro-Jade C-stained cells per square millimeter in the cingulate cortex and retrosplenial cortex. For each brain, data from three consecutive sections (50 μm thick) near the P6 #16 brain section (Paxinos et al., 2007) were averaged for the cingulate cortex and data from three consecutive sections (50 μm thick) near the P6#26 (Paxinos et al., 2007) were averaged for the retrosplenial cortex, and four to six brains per treatment group were analyzed.

All photomicrographs were taken through a 4X, 10X, or 40X objective with a Nikon Eclipse TE2000 inverted microscope attached to a digital camera DXM1200F.

Immunoblotting

Samples (the cortex, cerebellum, hippocampus, inferior colliculus, and forebrain) were homogenized (20% w/v) in ice cold Tris-HCl (20 mM, pH 7.4) buffer containing 1% Triton X-100, 1mM EGTA, 1 mM EDTA, 20 mM NaF, 1 mM Na-orthovanadate, 20 mM β-glycerophosphate, 5 μM microcystin, and 1μl/ml protease inhibitor cocktail (all from Sigma), and centrifuged at 52Kx g for 30 min. Samples (50 μg protein each) were boiled in SDS-sample buffer, separated on 10% or 15% SDS-PAGE, and blotted onto PVDF membranes. The membranes were then blocked with 5% nonfat dry milk and probed with rabbit monoclonal anti-cleaved caspase-3 antibody, mouse monoclonal anti-cleaved tau antibody, and mouse monoclonal tau-5 antibody (Millipore) as described previously (Saito et al., 2007a). Mouse monoclonal anti-β actin antibody (loading control, Abcam Inc. Cambridge, MA, USA) was always included. Antigens were detected by the Odyssey infrared imaging system using secondary antibodies, IR dye 680 conjugated goat anti-rabbit IgG (Invitrogen, Carlsbad, CA, USA) and IR dye 800 conjugated goat anti-mouse IgG (Rockland Immunochemicals, Gilbertsville, PA, USA). The amount of protein was measured by a BCA method (Pierce, Rockford, IL, USA).

Serine palmitoyltransferase assay

SPT activity was measured according to the methods of Rutti et al. (2009) and Diago et al. (2008). In brief, forebrain samples were homogenized in 0.32 M sucrose containing 2.5 mM EDTA, 1mM DTT and 50 mM HEPES buffer (PH 8.0), and the microsomal fractions were prepared. 250 μg of microsomal protein suspended in 100 mM HEPES (pH 8.0), 2.5 mM EDTA, 1.0 mM DTT and 0.1% sucrose monolaurate were incubated with 1.0 mM serine containing 0.2 μCi of L-[U-^{14}C] serine (50 μCi/ml), 0.2 mM palmitoyl CoA, and 50 μM pyridoxal 5'-phosphate in a total volume of 100 μl for 60 minutes at 37°C . For negative control, 2 μl ISP-1 solution (1 mg/ml in methanol) was added into the reaction mixture. Reaction was terminated by adding 500 μl of freshly prepared mixture of methanol/KOH: chloroform (4:1 v/v), and 25 μg of spinganine base in 10 μl chloroform (Kang et al., 2009) was added as a carrier. Non incorporated radiolabel (^{14}C serine) was removed by repeated alkaline water extraction. The chloroform extract was transferred to scintillation vial, evaporated to dryness, and radioactivity was measured in a liquid scintillation counter using Dimiscint (National Diagnostics, Sommerville, NJ, USA).Values are expressed as pmoles/mg/min.

Statistics

Values in a Table and Figures are expressed as mean ± Standard Error of Mean (SEM) obtained from 4–10 samples. Statistical analysis of the data was performed by two-tailed Student's *t* test and ANOVA with Bonferroni's post hoc test using the SPSS 11.0 program. A p value of <0.05 was considered significant.

Results

Brain regional differences in ethanol-induced caspase-3 activation

The increased expression of CC3 was observed in various brain regions of P7 mice 8 h after the first ethanol injection (Fig.1A), confirming previous studies (Olney et al, 2002;Dikraninan et al., 2005;Saito et al., 2007b). CC3 was strongly expressed in the cortex, thalamus, caudate putamen, and inferior colliculus, while it was expressed weakly in the cerebellum. Morphological observation indicated predominant neuronal localization of CC3 as reported previously (Olney et al, 2002;Saito et al., 2007b). Ethanol-induced caspase-3 activation was also assessed by the expression of Ctau, which is mainly produced by caspase-3 and highly expressed in degenerating axons/dendrites (Saito et al., 2010). As shown in Fig. 1B, Ctau expression was high in the cortex, hippocampus, and inferior colliculus, and low in the cerebellum. In agreement with the immunohistochemical studies, immunoblot results in Fig. 1C and D showed that ethanol significantly increased CC3 levels in the cortex, hippocampus, and inferior colliculus, while no significant changes were observed in the cerebellum. The ethanol-induced increase in Ctau in the cerebellum was significant, but the level of Ctau in ethanol-treated samples was less than 15% of those in other brain regions. The amounts of total caspase-3 were similar among these brain regions including cerebellum, although total tau recognized by anti-tau 5 antibody was significantly less (about 50% of other brain regions) in the cerebellum.

Ethanol-induced alterations in lipid levels in the cortex, cerebellum, hippocampus, and inferior colliculus

Twenty-four hours after P7 mice were exposed to ethanol under the conditions that induce neurodegeneration in many brain areas as described above, levels of ceramide (Fig. 2A), TG (Fig. 2B), NAPE (Fig. 2C), and ChE (Fig. 2D) were examined in the cortex (CX), cerebellum (CB), hippocampus (HIP), and inferior colliculus (IC). As previously reported in the whole brain (Saito et al., 2007a), ethanol induced significant elevations in ceramide, TG,

NAPE, and ChE in the cortex, hippocampus, and inferior colliculus. However, levels of ceramide and TG in the cerebellum were not significantly changed. Also, the level of NAPE in the cerebellum treated with ethanol was less than 9% of those in the cortex, hippocampus, and inferior colliculus. In contrast, significant increases in ChE were observed in all brain regions examined. Thus, results shown in Figures 1 and 2 suggest that increases in ceramide, TG, and NAPE are associated with ethanol-induced neurodegeneration.

As shown in Fig.1, ethanol-induced caspase-3 activation in the cerebellum was minimal at P7. However, ethanol triggered significant caspase-3 activation (3.4 ± 0.49 fold, $p<0.05$ by Student's *t* test) and a significant ceramide elevation (0.20 ± 0.05 μg/mg protein in the control and 0.45 ± 0.06 μg/mg protein in the ethanol group, $p<0.05$ by Student's *t* test) in the P4 cerebellum. This observation also suggests the correlation between caspase-3 activation and ceramide elevation.

The effects of SPT inhibitors on lipid metabolism and caspase-3 activation in the P7 mouse brain

In order to evaluate the involvement of ceramide in the ethanol-induced apoptotic pathway, P7 mice were injected via icv with an SPT inhibitor, ISP-1, 1 h before ethanol injections, and the brain lipids were analyzed 24 h after the ethanol injection (Table 1). Results showed that ISP-1 reduced ceramide levels in the presence and absence of ethanol, and there were no significant differences between the ISP-1 group and the ethanol+ISP-1 group. ISP-1 also blocked ethanol-induced accumulation of NAPE and ChE. However, TG levels were not significantly changed between the ethanol and the etanol+ISP-1 groups. The slight reduction of SM and GD1a (the most abundant ganglioside in the P7 mouse brain) by ISP-1 did not reach a significant level. LCS, another SPT inhibitor, injected via icv1 h before ethanol exposure also affected ceramide levels 8 h after the first ethanol exposure: 52 ± 4.8 (mean ± SEM ng/mg wet weight in the saline group), 32.2 ± 4.8 (in LCS group), 76.7 ± 8.7 (in ethanol group), and 49.5 ± 2.1 (in ethanol+LCS group). LCS reduced basal and ethanol-enhanced ceramide levels significantly (by ANOVA with Bonferroni's post hoc test, $p=0.05$ and $p=0.01$, respectively). TG levels were: 218 ± 22.9 (mean ± SEM ng/mg wet weight in the saline group), 210 ± 35.2 (in LCS group), 328 ± 42.5 (in ethanol group), and 373 ± 34.1 (in ethanol+LCS group). Although TG amounts were significantly augmented by ethanol (by ANOVA with Bonferroni's post hoc test, $p=0.01$), there was no significant difference between the ethanol group and the ethanol+LCS group.

Pretreatment with ISP-1 under the same conditions significantly attenuated ethanol-induced caspase-3 activation detected by immunoblotting with anti-CC3 and anti-Ctau antibodies, although ISP-1 did not suppress ethanol-induced caspase-3 activation completely (Fig. 3A, B). Reduction in ethanol-induced caspase-3 activation by ISP-1 was also confirmed by immunohistochemistry (Fig. 3C). LCS similarly attenuated ethanol-induced caspase-3 activation in P7 brains either via ip (Fig. 3D and E) or via icv injections (Fig. 3F). These results suggest that *de novo* ceramide synthesis is involved in the ethanol-induced apoptotic pathway. We further examined whether LCS attenuates ethanol-induced neurodegeneration assessed by Fluoro-Jade C staining. As shown in Fig. 4, strong Fluoro-Jade (FJ) staining observed in the cingulate cortex and the retrosplenial cortex of ethanol-treated mice was significantly attenuated by LCS treatment.

Cellular localization of SPT in the P7 mouse brain treated with ethanol

We next examined the cellular localization of SPT, which initiates *do novo* sphingolipid synthesis. P7 mice were injected with saline (Ctr) or ethanol (Eth), and brain sections were dual-labeled with the anti-SPT antibody and the anti-NeuN antibody (Fig. 5A). In the control brain, SPT was expressed uniformly in NeuN-positive neurons (Ctr 8h). However, in

the ethanol-treated brain, strong SPT expression was observed in certain NeuN-positive neurons 8 h after ethanol injection (Eth 8h), and by 24 h most of the strong expression of SPT appeared to be localized in degenerating projections (Eth 24h). Dual-labeling with anti-SPT and anti-CC3 antibodies revealed that strong SPT expression observed in neurons 8 h after ethanol exposure was overlapped with CC3 expression (Fig. 5B). The predominant localization of SPT in neurons and the strong expression of SPT in CC3-positive neurons suggest that ethanol-induced ceramide elevation occurs in neurons through the regulation of SPT. While significant differences in SPT expression were not detected between saline-treated and ethanol-treated forebrain samples by immunoblot analyses, small but significant increases in SPT activities (control: 4.85 ± 0.06 pmoles/mg/min; ethanol: 5.3 ± 0.37 pmoles/mg/min) were observed in ethanol-treated forebrain samples.

Discussion

The present study strongly indicates the involvement of ceramide and SPT in ethanol-induced apoptotic neurodegeneration in the P7 mouse brain. First, we demonstrated that the cerebellum, which was relatively resistant to ethanol exposure and showed little caspase-3 activation at P7, did not exhibit any significant ceramide elevation, while the cortex, hippocampus, and inferior colliculus, which showed substantial caspase-3 activation by ethanol, manifested significant ceramide elevation (Fig. 1 and 2). However, ethanol-induced increases in NAPE and TG were also much less (or insignificant) in the cerebellum compared to other brain regions examined (Fig. 2). Our previous time course studies using whole brain samples showed that the ethanol-induced TG elevation preceded the ceramide elevation (Saito et al., 2007a), and our present study demonstrated that an SPT inhibitor (ISP-1), which blocked ethanol-induced caspase-3 activation (Fig. 3A-C) and elevations in ceramide, NAPE, and ChE, did not block the TG elevation (Table 1). Also, LCS, another SPT inhibitor, which attenuated ethanol-induced ceramide elevation and caspase-3 activation (Fig. 3D-F), did not block the TG elevation. These studies imply that TG elevation is not directly involved in the induction of apoptosis, although it may indicate the enhancement of lipogenesis by ethanol, leading to ceramide elevation as previously proposed (Saito et al., 2007a). On the other hand, the ethanol-induced elevation in NAPE occurs later than the ceramide elevation and caspase-3 activation (Saito et al., 2007a), suggesting that the accumulation of NAPE may be more relevant to the progression rather than the initiation of the apoptotic process. Increases in NAPE have been associated with neurodegeneration induced by several insults such as concussion head trauma and NMDA-induced excitotoxicity (Hansen et al., 2001). In contrast to ceramide, TG, and NAPE, ethanol-induced elevation in ChE was observed in all brain regions examined.

Although we found that the cerebellum is less vulnerable to ethanol compared to the cortex, hippocampus, and inferior colliculus at P7, previous studies have indicated that the cerebellum is more sensitive to ethanol during the early neonatal period (Dikraninan et al., 2005; Siler-Marsiglio et al. 2006). In agreement with the reports, we found that ethanol induced significant caspase-3 activation and ceramide elevation in the P4 mouse brain.

Our results demonstrate that SPT inhibitors, along with inhibition of ceramide formation (Table 1), effectively blocked ethanol-induced caspase-3 activation (Fig. 3) and the subsequent neurodegeneration (Fig.4), suggesting that ceramide, which is considered a pro-apoptotic agent, triggers ethanol-induced apoptotic process in the P7 mouse brain. However, we cannot rule out the possibility that some other sphingolipids are also involved in apoptosis. In our previous studies (Saito et al., 2007a), we have shown that the amounts of brain gangliosides, such as GD1a, in the ethanol-treated group were higher than those in the saline group, when P7 mice were kept in the absence of the dams for 24 h after ethanol exposure. In the present study, GD1a was not significantly affected by ethanol (Table 1),

probably because pups were kept with dams, and some lipids were differentially affected by ethanol in the presence and absence of dams (Saito et al., 2007a). However, even in the presence of dams, some gangliosides, such as GM2, were increased by ethanol treatment (data not shown), and other sphingolipid metabolites, such as sphingosine and sphingosine 1-phosphate, were also affected by ethanol (manuscript in preparation). The effects of SPT inhibitors on these sphingolipids remain to be elucidated. SPT inhibitor experiments (Table 1) also indicate that *de novo* ceramide synthesis, where SPT acts as a rate-limiting enzyme, is essential for the ceramide elevation triggered by ethanol, although concurrent involvement of other pathways for ceramide accumulation, such as the sphingomyelin pathway (Hannun, 1996) and the salvage pathway (Kitatani et al., 2008), cannot be excluded. Possible activation of these pathways other than *de novo* ceramide synthesis may be a reason why SPT inhibitors did not suppress ethanol-induced caspase-3 activation completely (Fig. 3B, E), although it is possible that some other pathways unrelated to ceramide metabolism are also involved in ethanol-induced apoptotic neurodegeneration. Our previous study using cultured neurons indicated the importance of *de novo* ceramide synthesis in ethanol-induced apoptosis (Saito et al., 2005). Likewise, experiments by others using SPT inhibitors indicate involvement of *de novo* ceramide synthesis in various apoptotic pathways such as retinoic acid-induced apoptosis in PCC7-Mz1 cells (Herget et al., 2000), Aβ-induced toxicity in hippocampal neurons (Cutler et al., 2004), oxidative and excitotoxic insults in motor neurons (Cutler et al., 2002), and hypoxia-induced apoptosis in SHSY5Y cells (Kang et al., 2009). However, these studies have been performed using *in vitro* culture systems. Our present study has demonstrated that SPT inhibitors can be successfully utilized to reduce ceramide levels and to alleviate apoptosis triggered by ethanol *in vivo* in the brain. Such *in vivo* studies have been rarely described previously, although LCS has been applied to an animal model of globoid cell leukodystrophy as a substrate reduction intervention (LeVine et al., 2000).

It is possible that neuroprotective effects of SPT inhibitors found in our studies may not be mediated through the inhibition of SPT, because these inhibitors appear to have other functions as well (Osuchowski et al., 2004; Fenn et al., 2005). Experiments using siRNA against SPT may be useful to exclude such possibility. Nevertheless, our results showing that SPT was mainly localized in neurons and expressed robustly in apoptotic neurons in ethanol-treated brains (Fig. 5) strongly indicate the involvement of SPT in the apoptotic process. Neuronal localization of SPT is consistent with a previous study (Batheja et al., 2003). The cellular and subcellular localization of ceramide increased by ethanol is now under investigation.

Collectively, our data indicate importance of SPT and *de novo* ceramide synthesis in ethanol-induced apoptotic neurodegeneration in the developing brain. Neuroprotection by SPT inhibitors suggests SPT or other steps of *de novo* ceramide synthesis as possible therapeutic targets for alleviating ethanol toxicity in the developing brain.

Acknowledgments

This work was supported by an NIH/NIAAA grant R01 AA015355.

Abbreviations

FASD	fetal alcohol spectrum disorders
P7	postnatal day 7
TG	triglyceride

ChE	cholesterol ester
NAPE	N-acylphosphatidylethanolamine
CC3	cleaved caspase-3
Ctau	caspase-cleaved tau
SPT	serine palmitoyltransferase
LCS	L-cycloserine
icv	intracerebroventricular
ip	intraperitoneal
HPTLC	high-performance thin layer chromatography
SM	sphingomyelin

References

Batheja AD, Uhlinger DJ, Carton JM, Ho G, D'Andrea MR. Characterization of serine palmitoyltransferase in normal human tissues. J Histochem Cytochem. 2003; 51:687–696. [PubMed: 12704216]

Carloni S, Mazzoni E, Balduini W. Caspase-3 and calpain activities after acute and repeated ethanol administration during the rat brain growth spurt. J Neurochem. 2004; 89:197–203. [PubMed: 15030404]

Cutler RG, Kelly J, Storie K, Pedersen WA, Tammara A, Hatanpaa K, Troncoso JC, Mattson MP. Involvement of oxidative stress-induced abnormalities in ceramide and cholesterol metabolism in brain aging and Alzheimer's disease. Proc Natl Acad Sci USA. 2004; 101:2070–2075. [PubMed: 14970312]

Cutler RG, Pedersen WA, Camandola S, Rothstein JD, Mattson MP. Evidence that accumulation of ceramides and cholesterol esters mediates oxidative stress-induced death of motor neurons in amyotrophic lateral sclerosis. Ann Neurol. 2002; 52:448–457. [PubMed: 12325074]

Daigo M, Arai Y, Oshida K, Kitamura Y, Hayashi M, Shimizu T, Yamashiro Y. Effect of hypoxic-ischemic injury on serine palmitoyltransferase activity in the developing rat brain. Pathobiology. 2008; 75:330–334. [PubMed: 19096228]

Dikranian K, Qin YQ, Labruyere J, Nemmers B, Olney JW. Ethanol-induced neuroapoptosis in the developing rodent cerebellum and related brain stem structures. Brain Res Dev Brain Res. 2005; 155:1–13.

Fenn TD, Holyoak T, Stamper GF, Ringe D. Effect of a Y265F mutant on the transamination-based cycloserine inactivation of alanine racemase. Biochemistry. 2005; 44:5317–5327. [PubMed: 15807525]

Goswami R, Dawson G. Does ceramide play a role in neural cell apoptosis? J Neurosci Res. 2000; 60:141–149. [PubMed: 10740218]

Han JY, Jeong JY, Lee YK, Roh GS, Kim HJ, Kang SS, Cho GJ, Choi WS. Suppression of survival kinases and activation of JNK mediate ethanol-induced cell death in the developing rat brain. Neurosci Lett. 2006; 398:113–117. [PubMed: 16414187]

Hannun YA. Functions of ceramide in coordinating cellular responses to stress. Science. 1996; 274:1855–1859. [PubMed: 8943189]

Hansen HH, Ikonomidou C, Bittigau P, Hansen SH, Hansen HS. Accumulation of the anandamide precursor and other N-acylethanolamine phospholipids in infant rat models of in vivo necrotic and apoptotic neuronal death. J Neurochem. 2001; 76:39–46. [PubMed: 11145976]

Herget T, Esdar C, Oehrlein SA, Heinrich M, Schutze S, Maelicke A, van Echten-Deckert G. Production of ceramides causes apoptosis during early neural differentiation in vitro. J Biol Chem. 2000; 275:30344–30354. [PubMed: 10862608]

Ikonomidou C, Bittigau P, Ishimaru MJ, Wozniak DF, Koch C, Genz K, Price MT, Stefovska V, Horster F, Tenkova T, Dikranian K, Olney JW. Ethanol-induced apoptotic neurodegeneration and fetal alcohol syndrome. Science. 2000; 287:1056–1060. [PubMed: 10669420]

Jana A, Hogan EL, Pahan K. Ceramide and neurodegeneration: susceptibility of neurons and oligodendrocytes to cell damage and death. J Neurol Sci. 2009; 278:5–15. [PubMed: 19147160]

Kang MS, Ahn KH, Kim SK, Jeon HJ, Ji JE, Choi JM, Jung KM, Jung SY, Kim DK. Hypoxia-induced neuronal apoptosis is mediated by de novo synthesis of ceramide through activation of serine palmitoyltransferase. Cell Signal. 2009; 22:610–618. [PubMed: 19932170]

Kitatani K, Idkowiak-Baldys J, Hannun YA. The sphingolipid salvage pathway in ceramide metabolism and signaling. Cell Signal. 2008; 20:1010–1018. [PubMed: 18191382]

Ledeen, RW.; Yu, RK. Gangliosides: structure, isolation, and analysis. In: Ginsburg, V., editor. Methods in Enzymology. Vol. 83. Academic Press; New York: 1982. p. 139-191.

LeVine SM, Pedchenko TV, Bronshteyn IG, Pinson DM. L-cycloserine slows the clinical and pathological course in mice with globoid cell leukodystrophy (twitcher mice). J Neurosci Res. 2000; 60:231–236. [PubMed: 10740228]

Nakamura K, Handa S. Coomassie brilliant blue staining of lipids on thin-layer plates. Anal Biochem. 1984; 142:406–410. [PubMed: 6084960]

Olney JW, Tenkova T, Dikranian K, Qin YQ, Labruyere J, Ikonomidou C. Ethanol-induced apoptotic neurodegeneration in the developing C57BL/6 mouse brain. Brain Res Dev Brain Res. 2002; 133:115–126.

Osuchowski MF, Johnson VJ, He Q, Sharma RP. Myriocin, a serine palmitoyltransferase inhibitor, alters regional brain neurotransmitter levels without concurrent inhibition of the brain sphingolipid biosynthesis in mice. Toxicol Lett. 2004; 147:87–94. [PubMed: 14700532]

Rutti MF, Richard S, Penno A, von Eckardstein A, Hornemann T. An improved method to determine serine palmitoyltransferase activity. J Lipid Res. 2009; 50:1237–1244. [PubMed: 19181628]

Paxinos, G.; Halliday, G.; Watson, C.; Koutcherov, Y.; Wang, HQ. Atlas of the developing brain at E17.5, P0, and P6. Academic Press; Burlington, MA: 2007.

Pettus BJ, Chlfant CE, Hannun YA. Ceramide in apoptosis: an overview and current perspectives. Biochim Biophys Acta. 2002; 1585:114–125. [PubMed: 12531544]

Sadakata T, Washida M, Iwayama Y, Shoji S, Sato Y, Ohkura T, Katoh-Semba R, Nakajima M, Sekine Y, Tanaka M, Nakamura K, Iwata Y, Tsuchiya KJ, Mori N, Detera-Wadleigh SD, Ichikawa H, Itohara S, Yoshikawa T, Furuichi T. Autistic-like phenotypes in Cadps2-knockout mice and aberrant CADPS2 splicing in autistic patients. J Clin Invest. 2007; 117:931–943. [PubMed: 17380209]

Saito M, Benson EP, Saito M, Rosenberg A. Metabolism of cholesterol and triacylglycerol in cultured chick neuronal cells, glial cells, and fibroblasts: accumulation of esterified cholesterol in serum-free culture. J Neurosci Res. 1987; 18:319–325. [PubMed: 3694714]

Saito M, Chakraborty G, Mao RF, Wang R, Cooper TB, Vadasz C, Saito M. Ethanol alters lipid profiles and phosphorylation status of AMP-activated protein kinase in the neonatal mouse brain. J Neurochem. 2007a; 103:1208–1218. [PubMed: 17683484]

Saito M, Chakraborty G, Mao RF, Paik SM, Vadasz C, Saito M. Tau phosphorylation and cleavage in ethanol-induced neurodegeneration in the developing mouse brain. Neurochem Res. 2010; 35:651–659. [PubMed: 20049527]

Saito M, Mao RF, Wang R, Vadasz C, Saito M. Effects of gangliosides on ethanol-induced neurodegeneration in the developing mouse brain. Alcohol Clin Exp Res. 2007b; 31:665–674. [PubMed: 17374046]

Saito M, Saito M, Cooper TB, Vadasz C. Ethanol-induced changes in the content of triglycerides, ceramides, and glucosylceramides in cultured neurons. Alcohol Clin Exp Res. 2005; 29:1374–1383. [PubMed: 16131844]

Siler-Marsiglio KI, Madorsky I, Pan Q, Neeley AW, Shaw G, Heaton MB. Effects of acute ethanol exposure on regulatory mechanisms of Bcl-2-associated apoptosis promoter, Bad, in neonatal rat cerebellum: differential effects during vulnerable and resistant developmental periods. Alcohol Clin Exp Res. 2006; 30:1031–1038. [PubMed: 16737462]

Williams RD, Wang E, Merrill AH Jr. Enzymology of long-chain base synthesis by liver: characterization of serine palmitoyltransferase in rat liver microsomes. Arch Biochem Biophys. 1984; 228:282–291. [PubMed: 6421234]

Young C, Roth KA, Klocke BJ, West T, Holtzman DM, Labruyere J, Qin YQ, Dikranian K, Olney JW. Role of caspase-3 in ethanol-induced developmental neurodegeneration. Neurobiol Dis. 2005; 20:608–614. [PubMed: 15927478]

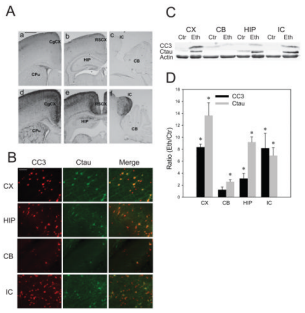

Fig. 1. Brain regional differences in ethanol-induced caspase-3 activation in the P7 mouse brain

A: Brain coronal (a, b, d, e) and sagittal (c, f) sections of mice sacrificed 8 h after saline (a, b, c) or ethanol (d, e, f) injections were immunostained by the anti-cleaved caspase-3 antibody.CgCX, cingulate cortex; CPu, caudate putamen; RSCX, retrosplenial cortex; HP, hippocampus; IC, inferior colliculus; CB, cerebellum. The bar indicates 500 μm. **B**: Brain coronal sections (the cingulate cortex region) of mice sacrificed 8 h after ethanol injections were dual-immunofluorescence labeled by anti-CC3 and anti-Ctau antibodies. CX, cortex; HIP, hippocampus; CB, cerebellum; IC, inferior colliculus. The bar indicates 500 μm. **C**: Immunoblots of the cortex (CX), cerebellum (CB), hippocampus (HIP), and inferior colliculs (IC) samples from mice sacrificed 8 h after saline (Ctr) or ethanol (Eth) injections were probed by anti-CC3, anti-Ctau, and anti-β actin antibodies. **D**: Quantitative analyses of CC3 and Ctau expression were performed using immunoblots, such as the one shown in **C**. Data (mean ± SEM, n=4) are expressed as ratios of protein band intensities in the ethanol (Eth) group to those in the control (Ctr) group after normalization to β-actin. *Significantly ($P < 0.05$) different between the ethanol and control groups by Student's *t*-test.

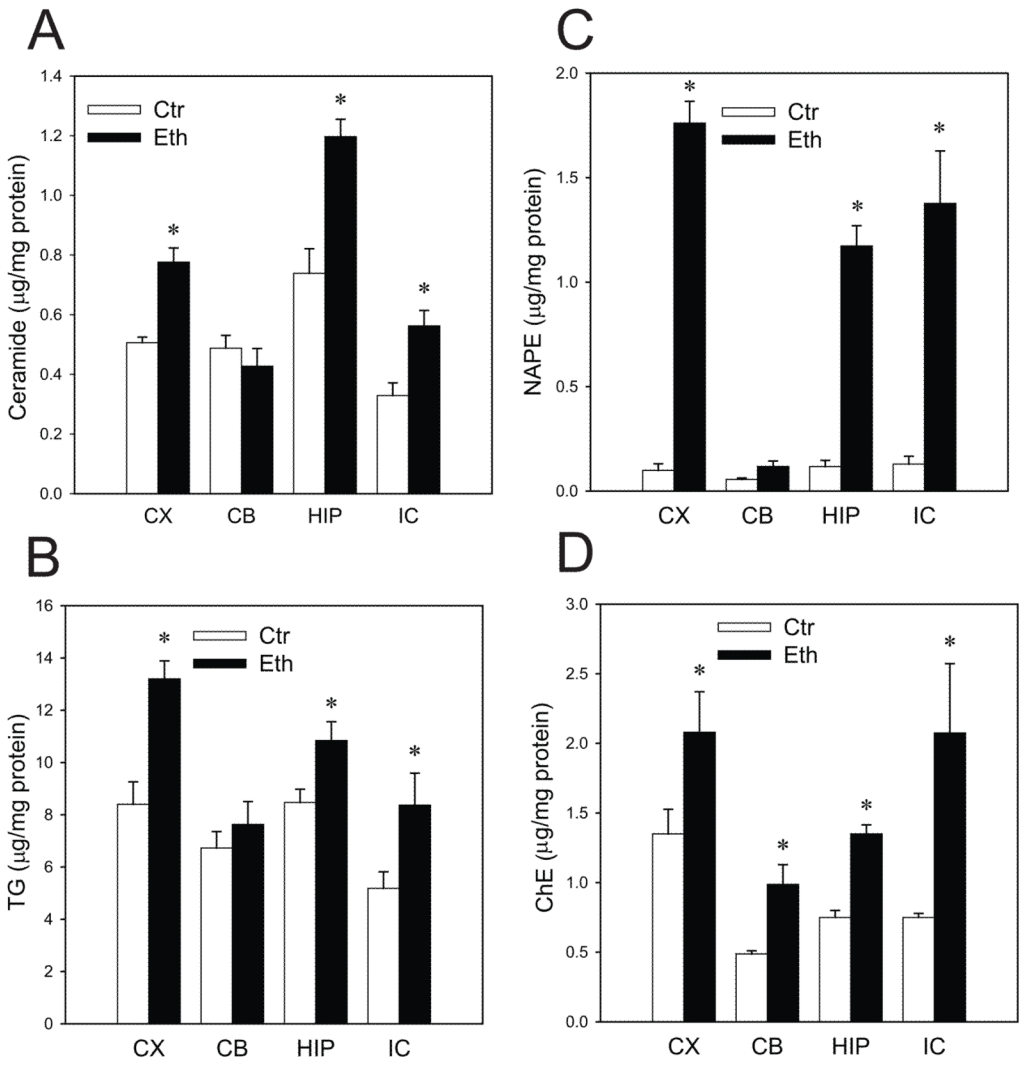

Fig. 2. Ethanol-induced alterations in lipid levels in the cortex, cerebellum, hippocampus, and inferior colliculus

The lipids extracted from the cortex (CX), cerebellum (CB), hippocampus (HIP), and inferior colliculus (IC) from the mice sacrificed 24 h after the first saline (Ctr) or ethanol (Eth) injections were separated on HPTLC, and the amounts of ceramide (**A**), TG (**B**), NAPE (**C**), and ChE (**D**) were measured as described in Materials and Methods. Values, presented as μg/mg protein, are mean ± SEM for four to six animals. *Significantly ($P < 0.05$) different between the ethanol and control groups by Student's *t*-test.

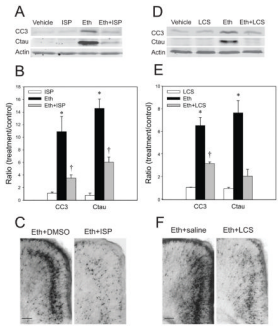

Fig. 3. The effects of SPT inhibitors on caspase-3 activation in the P7 mouse brain

A: Mice pretreated with ISP-1 or the vehicle were exposed to ethanol as described in Materials and Methods. Eight hours after ethanol exposure, forebrain samples from four groups, the vehicle only (Vehicle), ISP-1only (ISP), ethanol only (Eth), and ethanol+ISP (Eth+ISP) group, were collected and processed for immunoblotting to analyze CC3 and Ctau levels. A representative of such blots is shown here. **B**: Quantitative analyses of CC3 and Ctau levels by immunoblots in four groups described above in **A**. Data (mean ± SEM, n=4) are expressed as ratios of protein band intensities in the treatment (ISP, Eth, Eth+ISP) groups to those in the control (Vehicle) group after normalization to β-actin. *The value of ethanol group is significantly ($p< 0.05$) different from other groups, and †the value of Eth +ISP group is significantly ($p< 0.05$) different from ISP group, by ANOVA with Bonferroni's post hoc test. **C**: Mice pretreated with ISP-1 or the vehicle were exposed to ethanol, and brain sections of mice perfusion-fixed 8 h after ethanol treatment were stained with anti-CC3 antibody. The images show the cingulate cortex region. The bar indicates 100 μm. **D**: Mice injected with LCS or saline by ip were exposed to ethanol as described in Materials and Methods. Eight hours after ethanol exposure, forebrain samples from four groups, the vehicle only (Vehicle), LCS only (LCS), ethanol only (Eth), and ethanol+LCS (Eth+LCS) group, were collected and processed for CC3 and Ctau immunoblotting. A representative immunoblot is shown here. **E**: Quantitative analyses of CC3 and Ctau levels by immunoblots in four groups described above in **D**. Data (mean ± SEM, n=4) are expressed as ratios of protein band intensities in the treatment (LCS, Eth, Eth+LCS) groups to those in the control (Vehicle) group after normalization to β-actin. *The value of ethanol group is significantly ($p< 0.05$) different from other groups, and †the value of Eth+LCS group is significantly ($p< 0.05$) different from LCS group, by ANOVA with Bonferroni's post hoc test. **F**: Mice pretreated with saline or LCS (20 μg/2 μl) via icv were exposed to ethanol, and brain sections of mice perfusion-fixed 8 h after ethanol exposure were stained with anti-CC3 antibody. The images show the cingulate cortex region. The bar indicates 100 μm.

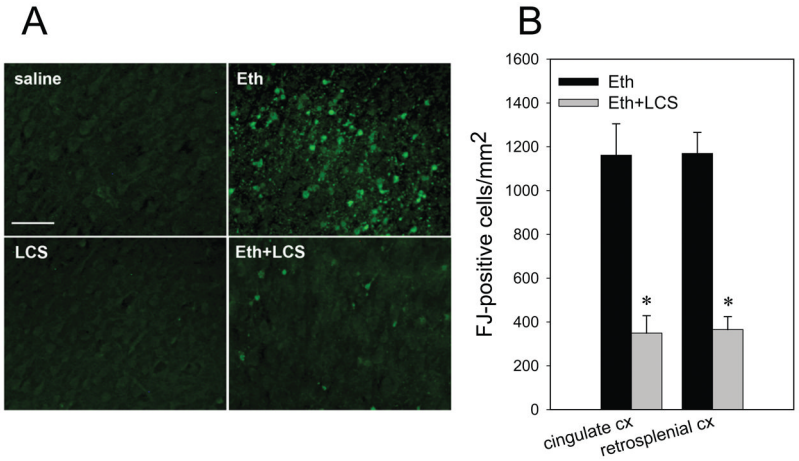

Fig. 4. The effects of LCS on ethanol-induced Fluoro-Jade C staining

A: Mice treated with LCS/saline via ip were exposed to ethanol/saline as described in Materials and Methods. Twenty four hours after ethanol/saline exposure, mice were perfusion-fixed, and brain sections from four groups, saline only (saline), LCS only (LCS), ethanol only (Eth), and ethanol+LCS (Eth+LCS) group, were stained with Fluoro-Jade C. The images show the cingulate cortex area. The bar indicates 50 μm. **B**: Fluoro-Jade C (FJ) positive cells were counted in the cingulate cortex (cingulate CX) and in the retrosplenial cortex (retrosplenial CX) as described in Materials and Methods. *Significantly ($p< 0.05$) different between the ethanol (Eth) and ethanol+LCS (Eth+LCS) groups by Student's *t*-test.

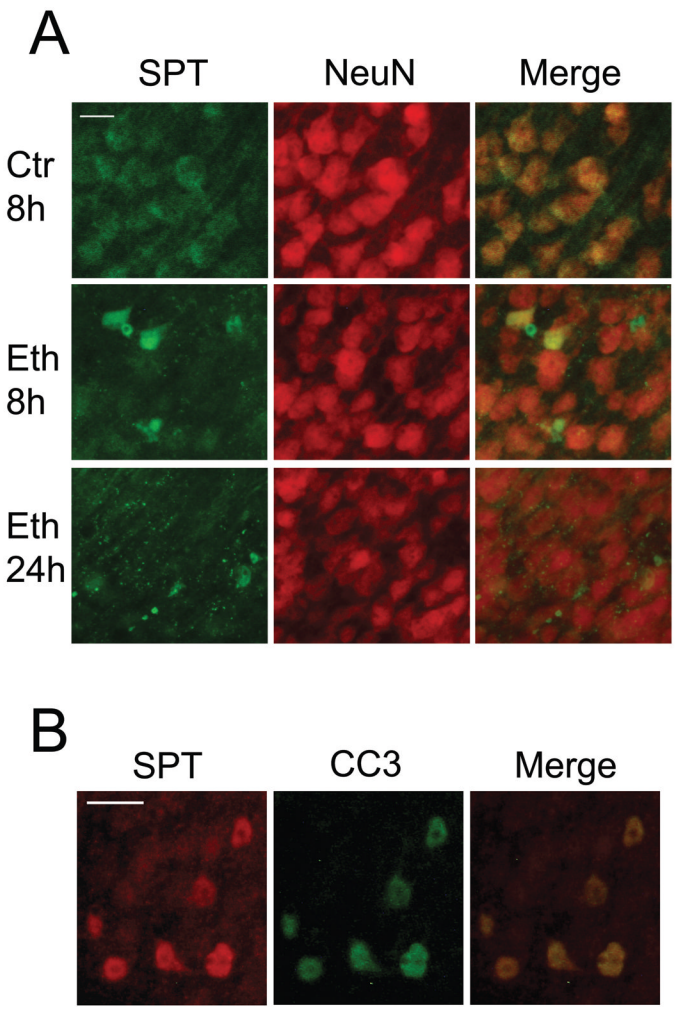

Fig. 5. Cellular localization of SPT in the P7 mouse brain treated with ethanol

A: Brain coronal sections (the cingulate cortex region) of mice sacrificed 8 h after the saline injection (Ctr 8h), 8 h after the ethanol injection (Eth 8h), and 24 h after the ethanol injection (Eth 24h) were dual-labeled by anti-SPT and anti-NeuN antibodies. The bar indicates 20 μm. **B**: Brain coronal sections (the cingulate cortex region) of mice sacrificed 8 h after the ethanol injection were dual-labeled by anti-SPT antibody and anti-CC3 antibody. The bar indicates 20 μm.

Table 1

Effects of ISP-1 on ethanol-induced alterations in lipid levels in P7 brains

Lipid	Vehicle	ISP-1	Ethanol	Ethanol+ISP-1
Ceramide	60.1 ± 6.1	38.7 ± 2.6	*84.7 ± 3.2	43.8 ± 2.2
TG	246 ± 9.1	256 ± 14.3	352 ± 28	319 ± 15
ChE	28 ± 6.0	20 ± 8.4	*123 ±18	76 ± 13
NAPE	16.3 ± 2.2	22.2 ± 2.5	*68.7 ± 7.1	38.3 ± 4.0
SM	444 ± 18	371 ± 45	422 ± 26	388 ± 24
GD1a	535 ± 26	474 ± 11	518 ± 8.3	467 ± 2.1

P7 mice were injected via icv with 2 μl of ISP-1 (1 μg/μl in saline containing 1% DMSO) or the vehicle. One hour after the injection, mice were injected subcutaneously twice (2 h apart) with saline or ethanol. Twenty-four hours after the first ethanol/saline injection, brains were removed for lipid analyses. Values, presented as ng/mg wet weight, are mean ± SEM (n=4).

* The value of ethanol group is significantly ($p<0.05$) different from all other groups by ANOVA with Bonferroni's post hoc test.